(article starts on next page)

# Atomic Layer Deposition of Buffer Layers for the Growth of Vertically Aligned Carbon Nanotube Arrays

Hao-Hao Li[1], Guang-Jie Yuan[1*], Bo Shan[1], Xiao-Xin Zhang[1], Hong-Ping Ma[2], Ying-Zhong Tian[3], Hong-Liang Lu[2] and Johan Liu[1,4]

## Abstract

Vertically aligned carbon nanotube arrays (VACNTs) show a great potential for various applications, such as thermal interface materials (TIMs). Besides the thermally oxidized $SiO_2$, atomic layer deposition (ALD) was also used to synthesize oxide buffer layers before the deposition of the catalyst, such as $Al_2O_3$, $TiO_2$, and ZnO. The growth of VACNTs was found to be largely dependent on different oxide buffer layers, which generally prevented the diffusion of the catalyst into the substrate. Among them, the thickest and densest VACNTs could be achieved on $Al_2O_3$, and carbon nanotubes were mostly triple-walled. Besides, the deposition temperature was critical to the growth of VACNTs on $Al_2O_3$, and their growth rate obviously reduced above 650 °C, which might be related to the Ostwald ripening of the catalyst nanoparticles or subsurface diffusion of the catalyst. Furthermore, the VACNTs/ graphene composite film was prepared as the thermal interface material. The VACNTs and graphene were proved to be the effective vertical and transverse heat transfer pathways in it, respectively.

**Keywords:** Atomic layer deposition, Vertically aligned carbon nanotube arrays, Oxide buffer layers, Thermal interface materials

## Background

Vertically aligned carbon nanotube arrays (VACNTs) have various outstanding performances and show great potential for a wide variety of applications. Due to their high axial thermal conductivity, many VACNT-based thermal interface materials (TIMs) have been developed for thermal packaging applications [1–7]. To synthesize the high-quality VACNTs on different substrates, chemical vapor deposition (CVD) has been commonly used, and the buffer layer should be deposited on the substrate before the deposition of the catalyst, such as Fe. Generally, the buffer layers are used to prevent the diffusion of the catalyst into substrates, so it is also very important to achieve the high-quality buffer layers on different substrates.

Atomic layer deposition (ALD) has self-limited behavior, which could achieve pinhole-free, dense, and conformal films on complex non-planar substrates [8].

Recently, many researchers have used it to deposit the buffer layers for the growth of VACNTs [9–11]. Amama et al. reported the water-assisted CVD of VACNTs using ALD Al as the buffer layer [9]. Quinton et al. reported the floating catalyst CVD of VACNTs using Fe as the catalyst. They found that VACNTs had faster nucleation rate and more uniform tube diameter on ALD $Al_2O_3$ buffer layer, compared with $SiO_2$ [10]. Compared with thermal and microwave plasma $SiO_2$, the VACNTs grown on ALD $SiO_2$ had the fastest nucleation rate [10]. Yang et al. reported that VACNTs could be synthesized on non-planar substrates using ALD $Al_2O_3$ as the buffer layer and $Fe_2O_3$ as the catalyst, respectively [11]. Compared with the planar surface, the non-planar surface could largely increase the specific surface area, which would be very beneficial for the preparation and further applications of VACNTs [12–14]. Although some ALD oxide buffer layers have been synthesized for the growth of VACNTs, their role was still not very clear in the CVD process.

* Correspondence: guangjie@shu.edu.cn
[1]SMIT Center, School of Automation and Mechanical Engineering, Shanghai University, Shanghai 201800, People's Republic of China
Full list of author information is available at the end of the article

**Fig. 1** Schematic diagram of the VACNTs/graphene composite film
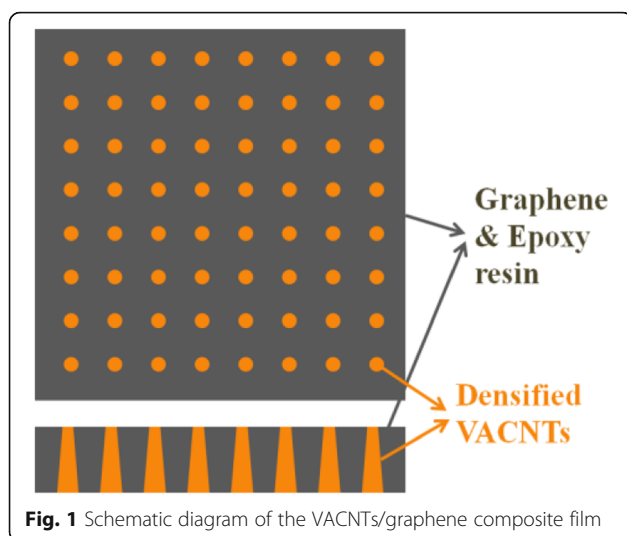
In this research, we used CVD to prepare the VACNTs with different buffer layers, including ALD $Al_2O_3$, ALD $TiO_2$, ALD ZnO, and thermally oxidized $SiO_2$. The effects of different oxide layers and deposition temperature on the growth of VACNTs were analyzed. Besides, the VACNTs/graphene composite film was also developed as the thermal interface material, and the VACNTs were used as the additional vertical thermal transfer pathways in it.

## Methods

$Al_2O_3$, ZnO, and $TiO_2$ thin films were deposited on Si substrates by ALD, and $SiO_2$ was formed on Si substrate by thermal oxidization. Trimethylaluminum (TMA), tetrakis(dimethylamino)titanium (TDMAT), and diethyl-zinc (DEZ) were used as the precursors for ALD of $Al_2O_3$, $TiO_2$, and ZnO films, respectively. For all of them, $H_2O$ was used as the oxygen source, and the deposition temperature was set at 200 °C. The thickness of $Al_2O_3$, ZnO, and $TiO_2$, and $SiO_2$ films was 20 nm. One-nanometer-thick Fe film was deposited on all of them by electron-beam (EB) evaporation, where it was used as the catalyst. The CVD method was applied to synthesize the VACNTs based on a commercial CVD system (AIXRON Black Magic II). Before the growth of VACNTs, the catalyst was annealed in the hydrogen ($H_2$) atmosphere at 600 °C. The period was 3 min, and the flow rate of $H_2$ was set at 700 sccm. After that, the acetylene ($C_2H_2$) and $H_2$ were introduced into the chamber, and then VACNTs were prepared. The flow rates of $C_2H_2$ and $H_2$ were 100 and 700 sccm, respectively. The deposition temperature was changed from 550 to 700 °C, and the period was fixed at 30 min.

After the growth of VACNTs on $Al_2O_3$, the VACNTs/graphene composite film was also prepared as the thermal interface material. Epoxy resin, curing agent, and diluents were purchased from Sigma-Aldrich Trading and Tokyo Chemical Industrial Co., Ltd. The multilayer graphene was purchased from Nanjing Xianfeng Nano-materials Technology Co., Ltd. For the preparation of the composite film, the catalyst was firstly patterned using a lithography machine (URE-2000S/A). The pattern size was 500 μm, and the distance was 150 μm among patterns. Secondly, the VACNTs were deposited by CVD at 650 °C, and the growth period was 30 min.
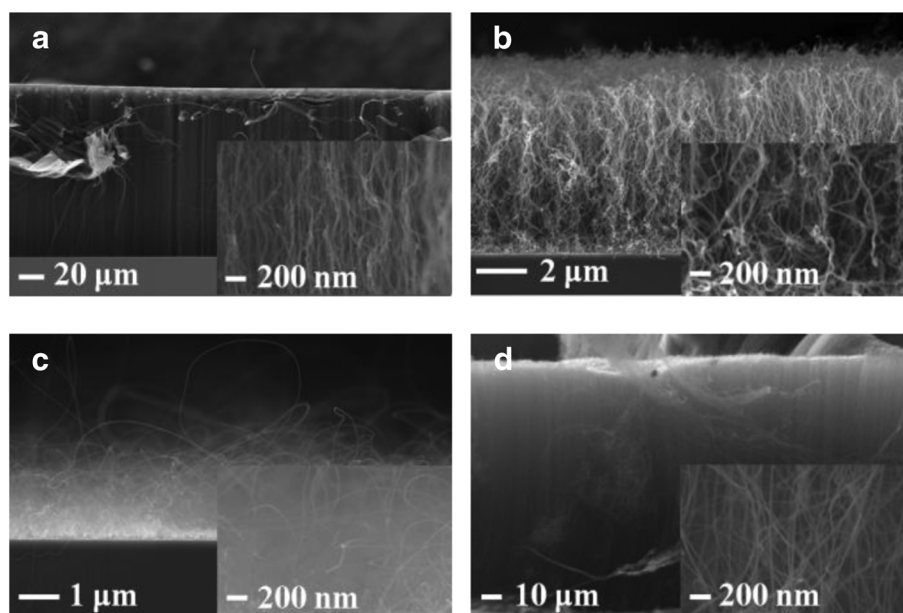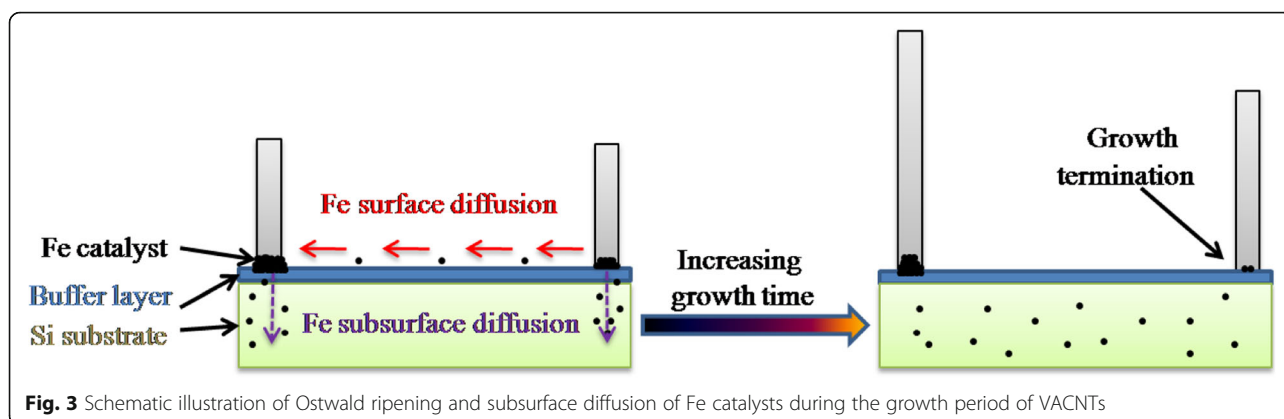


**Fig. 2** Cross-sectional SEM images of VACNTs grown on different oxide buffer layers at 650 °C: **a** $Al_2O_3$, **b** $TiO_2$, **c** ZnO, and **d** $SiO_2$

**Fig. 3** Schematic illustration of Ostwald ripening and subsurface diffusion of Fe catalysts during the growth period of VACNTs
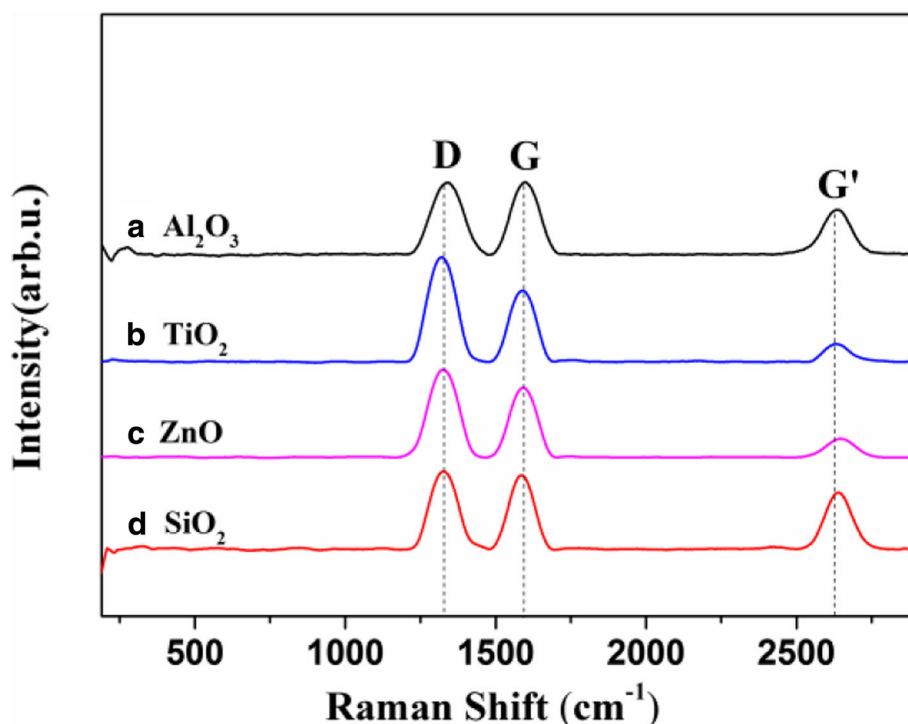
Thirdly, the VACNTs were densified by the acetone vapor, and the period was 20 s. Fourthly, graphene, epoxy resin, curing agent, and diluent were mixed as the matrix, and the amount of graphene was fixed at 10 wt.%. After that, the VACNTs were immersed into the matrix and cured in a vacuum oven at 120 °C for 1 h and then at 150 °C for 1 h. Finally, the prepared composite film was polished to the thickness of about 300 μm, and the tips of VACNTs should be protruded from its both surfaces, as shown in Fig. 1.

The morphology of VACNTs and the composite film was analyzed by the field emission scanning electron microscopy (FESEM, Merlin Compact) and transmission electron microscopy (TEM, Tecnai G2 F20 S-TWIN).

Raman spectra of VACNTs were recorded by inVia Reflex, using a laser excitation wavelength of 632.8 nm. The thermal diffusivity ($\alpha$) and specific heat capacity (Cp) of the composite film were measured by the laser flash thermal analyzer (Netzach LFA 467) and differential scanning calorimeter (DSC, Mettler Toledo DSC1), respectively. After that, the thermal conductivity could be calculated according to the Eq. 1:

$$\lambda = \alpha \times Cp \times \rho, \tag{1}$$

where $\lambda$ and $\rho$ were the thermal conductivity and density of the composite film, respectively.



**Fig. 4** Raman spectra of VACNTs grown on different buffer layers at 650 °C: **a** Al$_2$O$_3$, **b** TiO$_2$, **c** ZnO, and **d** SiO$_2$. The spectra have been normalized to the intensity of the G band in order to facilitate comparison

Li *et al. Nanoscale Research Letters*    (2019) 14:119
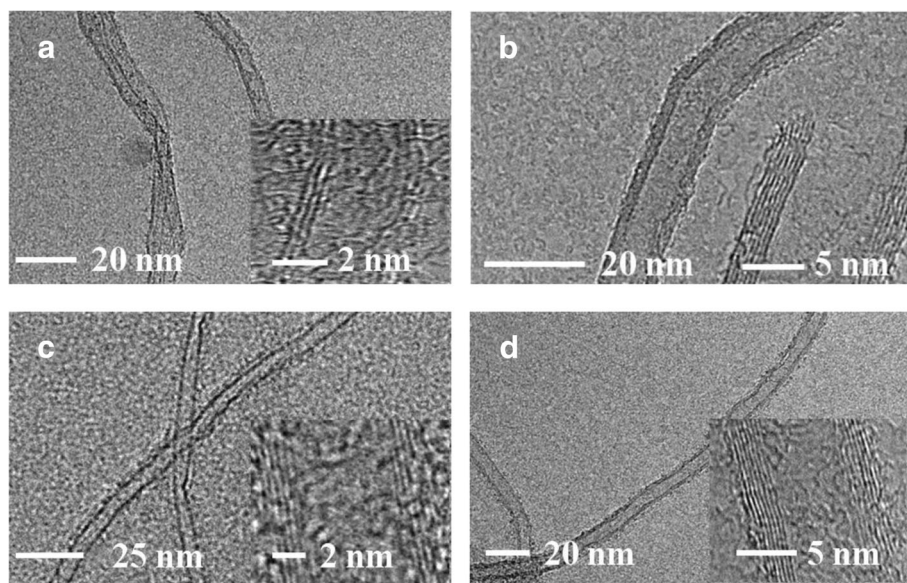
Page 4 of 7



**Fig. 5** TEM images of VACNTs grown on different buffer layers: **a** $Al_2O_3$, **b** $TiO_2$, **c** ZnO, and **d** $SiO_2$

## Results and Discussion

Figure 2 a–d show the cross-sectional SEM images of VACNTs grown on different oxide buffer layers at 650 °C. The VACNTs have been successfully prepared on $Al_2O_3$, $TiO_2$, and $SiO_2$, as shown in Fig. 2 a, b, and d. Among them, the VACNTs were the thickest on $Al_2O_3$, which indicated that the lifetime of catalyst nanoparticles was the longest on it during the growth period. The lifetime of catalyst nanoparticles represents the time after it has basically lost its catalytic function to grow carbon nanotubes, which could be deduced from the thickness of VACNTs [9]. Unlike it, the relatively thin VACNTs were deposited on $SiO_2$ and $TiO_2$, which might be caused by the relatively serious Ostwald ripening of catalyst nanoparticles or the subsurface diffusion of Fe [15, 16]. As shown in Fig. 3, Ostwald ripening is a phenomenon whereby larger nanoparticles increase in size while smaller nanoparticles, which have greater strain energy, shrink in size and eventually disappear via atomic surface diffusion [17]. When a catalyst nanoparticle disappeared, or when too much catalyst was lost, the carbon nanotubes growing from it stopped [17]. Besides, subsurface diffusion of Fe into the buffer layer or substrate could also cause mass loss from the catalysts that grow the carbon nanotubes, eventually causing termination of growth [16]. From Fig. 2 a, b, and d, we could also see that the density of VACNTs was the highest on $Al_2O_3$, and the lowest on $TiO_2$. Generally, any marginal alignment seen in CVD samples was due to a crowding effect, and carbon nanotubes supported each other by van der Waals attraction [18]. Therefore, it means that the density of VACNTS was quite important, and higher density generally resulted in better vertical alignment of VACNTs, which were confirmed in Fig. 2 a, b, and d. Besides, Fig. 2 c shows that there were almost no VACNTs grown on ZnO, which could be caused by much more serious Ostwald ripening of catalyst nanoparticles and subsurface diffusion of Fe, compared with others [15, 16].

Figure 4 a–d show Raman spectra of VACNTs grown on $Al_2O_3$, $TiO_2$, ZnO, and $SiO_2$. Generally, the D, G, and G' bands were around 1360 $cm^{-1}$, 1580 $cm^{-1}$, and 2700 $cm^{-1}$, respectively [19, 20]. For different oxide buffer layers, the ratio of $I_D$ and $I_G$ was calculated to be near or more than 1, and there were also no radial breathing modes (RBMs) around 200 $cm^{-1}$. It indicated that all the prepared VACNTs were multi-walled on $Al_2O_3$, $TiO_2$,
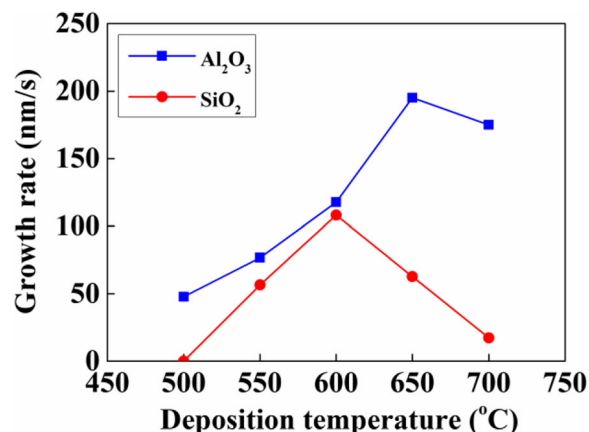


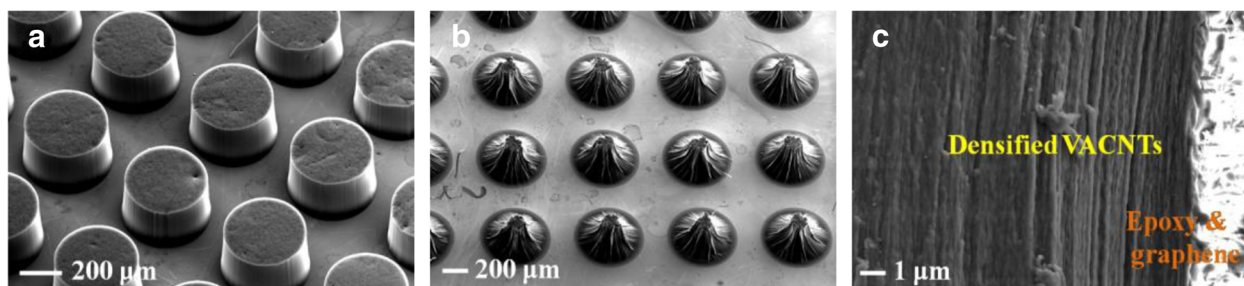**Fig. 6** The growth rate of VACNTs variation with deposition temperature on $Al_2O_3$ and $SiO_2$ buffer layers

**Fig. 7 a** The SEM image of VACNTs with the patterned catalyst. **b** The SEM image of VACNTs after the densification. **c** The cross-sectional SEM image of the VACNTs/graphene composite film

ZnO, and $SiO_2$. Figure 5 a–d show the morphology of VACNTs on different oxide buffer layers, which was analyzed by TEM. The VACNTs were multi-walled on all of them, which was consistent with the results of the Raman analysis. The VACNTs were mostly triple-walled on $Al_2O_3$, but more than four walls on $TiO_2$, ZnO, and $SiO_2$.

Figure 6 shows the growth rate of VACNT variation with deposition temperature on $Al_2O_3$ and $SiO_2$. When the temperature increased, the growth rate of VACNTs firstly raised and then decreased on both of them. It might be related to the serious Ostwald ripening of catalyst nanoparticles or subsurface diffusion of Fe, which largely reduced the lifetime of catalyst nanoparticles and the growth rate of VACNTs [15, 16]. Above 600 °C, the growth rate of VACNTs still increased on $Al_2O_3$, but decreased on $SiO_2$. It indicated that the lifetime of catalyst nanoparticles on $Al_2O_3$ was longer than that on $SiO_2$. When the deposition temperature was below 500 °C, there were obvious VACNTs on $Al_2O_3$ but no VACNTs on $SiO_2$, which meant that the nucleation and initial growth of VACNTs were more easily achieved on $Al_2O_3$, compared with $SiO_2$. It indicated that the activation energy for the nucleation and initial growth of VACNTs on $Al_2O_3$ was much lower than that on $SiO_2$. Commonly, each catalyst nanoparticle could produce at most one carbon nanotube, but not all the catalyst nanoparticles could achieve the carbon nanotubes, because the activation energy should be overcome for their nucleation and initial growth [21–23]. Therefore, compared with $SiO_2$, the lower activation energy of VACNTs on $Al_2O_3$ might result in their higher density, which could be confirmed by Fig. 2 a and d.

Figure 7 a shows the morphology of VACNTs with the patterned catalyst on $Al_2O_3$. Generally, there still had a lot of gaps inside VACNTs, which were filled with air, as shown in Fig. 2 a. However, the thermal conductivity of air was only 0.023 $Wm^{-1} K^{-1}$ at room temperature, so the VACNTs need to be densified to remove it. From Fig. 7 b, we could see that the obvious densification of VACNTs has been achieved with the acetone vapor. Figure 7 c shows the cross-sectional image of the VACNTs/graphene composite film. The VACNTs and graphene were used as the additional vertical and transverse thermal transfer pathways in it. Figure 8 a and b show the vertical and transverse thermal conductivities of the composite film, which were measured to be about 1.25 and 2.50 $Wm^{-1} K^{-1}$, respectively. Compared with the pure epoxy resin, its vertical and transverse thermal conductivities have been obviously enhanced. It confirmed that the effective vertical and transverse heat transfer pathways have been offered by the VACNTs and graphene in the composite film, respectively.
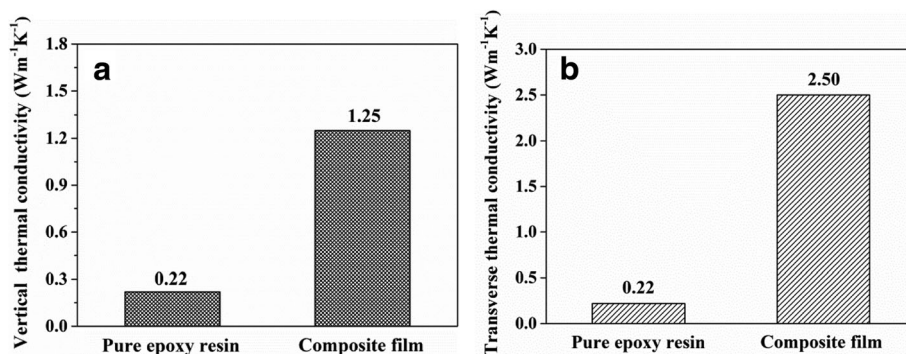


**Fig. 8** Thermal property of the VACNTs/graphene composite film: **a** the vertical thermal conductivity and **b** the transverse thermal conductivity

Li *et al. Nanoscale Research Letters*        (2019) 14:119

Page 6 of 7

## Conclusions

The growth of VACNTs has been analyzed on different oxide buffer layers, such as ALD $Al_2O_3$, ALD $TiO_2$, ALD ZnO, and thermally oxidized $SiO_2$. Among them, VACNTs were the thickest and densest on $Al_2O_3$, which indicated that the lifetime of catalyst nanoparticles was the longest and the vertical alignment of VACNTs was the best on it. Besides, the VACNTs were found to be multilayer on $Al_2O_3$, and the deposition temperature was very critical to the growth of VACNTs. Compared with $SiO_2$, the nucleation and initial growth of VACNTs were more easily achieved on $Al_2O_3$, which resulted in a higher density of VACNTs on it. After the growth of VACNTs on $Al_2O_3$, they were used to prepare the composite film together with graphene and epoxy resin. Compared with the pure epoxy resin, the vertical and transverse thermal conductivities of the composite film have been largely improved.

### Abbreviations

ALD: Atomic layer deposition; $C_2H_2$: Acetylene; CVD: Chemical vapor deposition; DEZ: Diethylzinc; DSC: Differential scanning calorimeter; EB: Electron-beam; FESEM: Field emission scanning electron microscopy; $H_2$: Hydrogen; LFA: Laser flash thermal analyzer; RBMs: Radial breathing modes; TDMAT: Tetrakis(dimethylamino)titanium; TEM: Transmission electron microscopy; TIMs: Thermal interface materials; TMA: Trimethylaluminum; VACNTs: Vertically aligned carbon nanotubes

### Availability of Data and Materials

The datasets supporting the conclusions of this article are included with the article.

### Authors' Contributions

HHL, GJY, BS, XXZ, and HPM designed the experiments and analyzed the data. HHL, GJY, BS, XXZ, HPM, YZT, HLL, and JL discussed the results and contributed to the writing of the manuscript. All authors read and approved the final manuscript.

### Competing Interests

The authors declare that they have no competing interests.

## Publisher's Note

Springer Nature remains neutral with regard to jurisdictional claims in published maps and institutional affiliations.

### Author details

$^1$SMIT Center, School of Automation and Mechanical Engineering, Shanghai University, Shanghai 201800, People's Republic of China. $^2$State Key Laboratory of ASIC and System, School of Microelectronics, Fudan University, Shanghai 200433, People's Republic of China. $^3$Shanghai Key Laboratory of Intelligent Manufacturing and Robotics, School of Automation and Mechanical Engineering, Shanghai University, Shanghai 200072, People's Republic of China. $^4$Electronics Materials and Systems Laboratory, Department of Microtechnology and Nanoscience, Chalmers University of Technology, SE-412 96 Goteborg, Sweden.

### References

1. Li L, Yang Z, Gao H, Zhang H, Ren J, Sun X, Chen T, Kia HC, Peng H (2011) Vertically aligned and penetrated carbon nanotube/polymer composite film and promising electronic applications. Adv Mater. 23:3730–3735
2. Wang CY, Chen TH, Chang SC, Cheng SY, Chin TS (2010) Strong carbon-nanotube-polymer bonding by microwave irradiation. Adv Funct Mater. 17:1979–1983
3. Peacock MA, Roy CK, Hamilton MC, Johnson RW, Knight RW, Harris DK (2016) Characterization of transferred vertically aligned carbon nanotubes arrays as thermal interface materials. Int J Heat Mass Tran. 97:94–100
4. Ping LQ, Hou PX, Liu C, Li JC, Zhao Y, Zhang F, Ma CQ, Tai KP, Cong HT, Cheng HM (2017) Surface-restrained growth of vertically aligned carbon nanotube arrays with excellent thermal transport performance. Nanoscale 9:8213–8219
5. Hao ML, Huang ZX, Saviers KR, Xiong GP, Hodson SL, Fisher TS (2017) Characterization of vertically oriented carbon nanotubes arrays as high-temperature thermal interface materials. Int J Heat Mass Tran. 106:1287–1293
6. Uetani K, Ata S, Tomonoh S, Yamada T, Yumura M, Hata K (2014) Elastomeric thermal interface materials with high through-plane thermal conductivity from carbon fiber fillers vertically aligned by electrostatic flocking. Adv Mater. 26:5857–5862
7. Wang M, Li TT, Yao YG, Lu HF, Li Q, Chen MH, Li QW (2014) Wafer-scale transfer of vertically aligned carbon nanotube arrays. J Am Chem Soc. 136:18156–18162
8. George SM (2010) Atomic layer deposition: an overview. Chem Rev. 110:111–131
9. Amama PB, Pint CL, Kim SM, Mcjilton L, Eyink KG, Stach EA, Hauge RH, Maruyama B (2010) Influence of alumina type on the evolution and activity of alumina-supported Fe catalysts in single-walled carbon nanotube carpet growth. Acs Nano 4:895–904
10. Quinton BT, Leedy KD, Lawson JW, Tsao B, Scofield JD, Merrett JN, Zhang Q, Yost K, Mukhopadhyay SM (2015) Influence of oxide buffer layers on the growth of carbon nanotube arrays on carbon substrates. Carbon 87:175–185
11. Yang C, Li Y, Yan L, Cao YZ (2016) Influence of catalyst film thickness deposited by atomic layer deposition on growth of aligned carbon nanotubes. J Inorg Mater. 31:681–686
12. Zhang Q, Huang JQ, Zhao MQ, Qian WZ, Wang Y, Wei F (2008) Radial growth of vertically aligned carbon nanotube arrays from ethylene on ceramic spheres. Carbon 46:1152–1158
13. Zhou K, Huang JQ, Zhang Q, Wei F (2010) Multi-directional growth of aligned carbon nanotubes over catalyst film prepared by atomic layer deposition. Nanoscale Res Lett. 5:1555–1560
14. Xiang R, Luo GH, Qian WZ, Wang Y, Wei F, Li Q (2007) Large area growth of aligned CNT arrays on spheres: towards large scale and continuous production. Chem Vapor Depos. 13:533–536
15. Navas H, Picher M, Ledier AA, Fossard F, Michel T, Kozawa A, Maruyama T, Anglaret E, Loiseau A, Jourdain V (2017) Unveiling the evolutions of nanotube diameter distribution during the growth of single-walled carbon nanotubes. ACS Nano 11:3081–3088
16. Kim SM, Pint CL, Amama PB, Zakharov DN, Hauge RH, Maruyama B, Stach EA (2010) Evolution in catalyst morphology leads to carbon nanotube growth termination. J Phys Chem Lett. 1:918–922
17. Amama PB, Pint CL, McJilton L, Kim SM, Stach EA, Murray PT, Hauge RH, Maruyam B (2009) Role of water in super growth of single-walled carbon nanotube carpets. Nano Lett. 9:44–49
18. Lee IH, Han GH, Chae SJ, Bae JJ, Kim ES, Kim SM, Kim TH, Jeong HK, Lee YH (2010) Criteria for producing yarns from vertically aligned carbon nanotubes. Nano 5:31–38
19. Kuznetsov VL, Bokova-Sirosh SN, Moseenkov SI, Ishchenko AV, Krasnikov DV, Kazakova MA, Romanenko AI, Tkachev EN, Obraztsova ED (2014) Raman spectra for characterization of defective CVD multi-walled carbon nanotubes. Phys Status Solidi B 251:2444–2450
20. Delosarcos T, Garnier MG, Oelhafen P, Mathys D, Seo JW, Domingo C, Vicente Garcia RJ, Sanchez CS (2004) Strong influence of buffer layer type on carbon nanotube characteristics. Carbon 42:187–190
21. Kharlamova MV (2017) Investigation of growth dynamics of carbon nanotubes. Beilstein J Nanotechnol. 8:826–856

22.  In JB, Grigoropoulos CP, Chernov AA, Noy A (2011) Growth kinetics of vertically aligned carbon nanotube arrays in clean oxygen-free condition. ACS Nano 5:9602–9610
23.  Chen GH, Davis RC, Kimura H, Sakurai S, Yumura M, Futaba DN, Hata K (2015) The relationship between the growth rate and the lifetime in carbon nanotube synthesis. Nanoscale 7:8873–8878